LONG-TERM PREDICTION OF LONGSHORE SEDIMENT TRANSPORT IN THE CONTEXT OF CLIMATE CHANGE

Amin Reza Zarifsanayei[*,1,2], Amir Etemad-Shahidi [1,2], Nick Cartwright[1,2], and Darrell Strauss[2]

Due to climate change impacts on atmospheric circulation, global and regional wave climate in many coastal regions around the world might change. Any changes in wave parameters could result in significant changes in wave energy flux, the patterns of coastal sediment transport, and coastal evolution. Although some studies have tried to address the potential impacts of climate change on longshore sediment transport (LST) patterns, they did not sufficiently consider the uncertainties arising from different sources in the projections. In this study, the uncertainty associated with the choice of model used for the estimation of LST is examined. The models were applied to a short stretch of coastline located in Northern Gold Coast, Australia, where a huge volume of sediment is transported along the coast annually. The ensemble of results shows that the future mean annual and monthly LST rate might decrease by about 11 %, compared to the baseline period. The results also show that uncertainty associated with LST estimation is significant. Hence, it is proposed that this uncertainty, in addition to that from other sources, should be considered to quantify the contribution of each source in total uncertainty. In this way, a probabilistic-based framework can be developed to provide more meaningful output applicable to long-term coastal planning.

Keywords: climate change; long-term impacts; longshore sediment transport

NTRODUCTION

Coastal areas are a major focus for the development of cities and infrastructure. Sandy coasts can act as natural barriers to protect coastal regions from inundation by storm surge and wave action. Sandy beach-dune systems evolve under the influence of many coastal processes that act across a wide range of spatio-temporal scales (Masselink and Hughes, 2003). Longshore processes are among the key factors controlling long-term shoreline changes (e.g., Ruggiero, 2010 Ruggiero et al., 2016; Antolínez et al., 2018). In this regard, changes in the patterns of longshore processes and the resulting shoreline changes can affect coastal communities worldwide. Longshore sediment transport (hereafter LST) gradient is essential for shoreline changes calculations, and is adopted as the basis of several shoreline models such as GENESIS (Hanson and Kraus, 1989), LITPACK (DHI, 2017), UNIBEST (Tonnon et al., 2018). The performance of the shoreline models depends directly on the accuracy of the methods used for estimation of LST rate along the shoreline. In coastal studies, estimates of LST can be obtained from field measurements or sediment transport models (e.g., empirical formulas, numerical models). Field measurements can provide qualitative and quantitative information on historic LST patterns. Nevertheless, they have some significant constraints (Cooper and Pilkey, 2007) and are costly. Empirical formulas simplify sediment transport phenomena through parametrization. However, direct use of empirical formulas without engineering judgments could lead to unreliable results. Numerical models simulate detailed hydrodynamic and sediment transport processes, but they should be calibrated against observations to provide reliable results. Additionally, the performance of the models directly depends on the fundamental assumptions behind the model development (e.g., initiation of sediment movements), as well as the forcing conditions (e.g., waves) under which the models are implemented.

Coastal management plans require quantitative and qualitative estimates of LST patterns in long-term scales (e.g., decades) (Magnor et al., 2017). On the other hand, any estimation in these time scales should account for potential climate change (hereafter CC) impacts on coastal sediment transport patterns and associated uncertainties (Ranasinghe, 2016). In this regard, a modeling framework is required to be calibrated against field measurements for a baseline period. Then the framework can be driven by future forcing conditions. Future forcing conditions, themselves, are explicitly dependent on the predictions of CC impacts on atmospheric circulations on global, regional, and local scales. Hence, each part of such a framework is influenced by uncertainties arising from different sources that could lead to highly uncertain projections. It should be pointed out that uncertainty in projection of future patterns of LST can be classified in two main categories: epistemic (knowledge) uncertainty, and intrinsic (aleatory) uncertainty (Toimil et al., 2020). A prime example of epistemic uncertainty (knowledge uncertainty) is

[*,1] School of Engineering and Built Environment, Griffith University, Gold Coast campus, Queensland, 4222 QLD, Australia. Email address: aminreza.zarifasanayei@griffithuni.edu.au

[2] Griffith Centre for Coastal Management , Griffith University, Gold Coast Campus, Queensland, 4222 QLD, Australia

the existence of a wide range of coastal sediment transport models developed under different assumptions. Variability of climate systems can be considered as aleatory/intrinsic uncertainty. Figure 1 illustrates the potential sources of uncertainty in the projection of LST patterns.

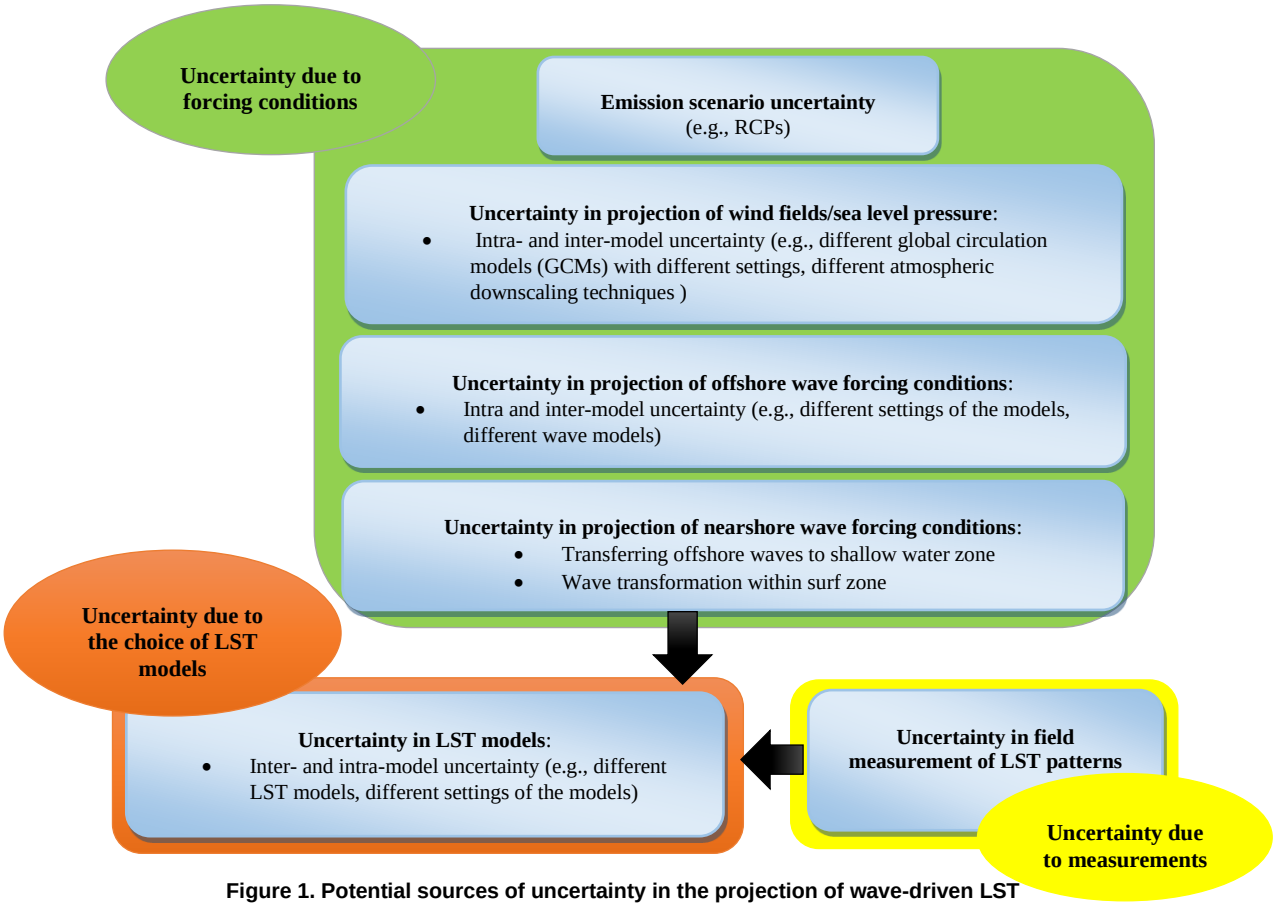

Figure 1. Potential sources of uncertainty in the projection of wave-driven LST

There have been some efforts to estimate future LST patterns for different case studies around the world (e.g., West Africa (Almar et al., 2015), Vietnam (Dastgheib et al., 2016), India (Chowdhury et al., 2020)). Nonetheless, they mainly addressed the uncertainty associated with global circulation models and/or emission scenarios, and they overlooked other sources of uncertainty. A reliable prediction of future LST rates requires addressing uncertainty associated with all sources. One of the main sources of uncertainty is the choice of LST estimation method. Two conventional models for estimation of LST are simplified (bulk transport formulae) and process-based models. In recent decades, many researchers endeavored to develop or modify formulas for the prediction of the LST rate (e.g., Mil-Homens et al., 2013; Shaeri et al., 2020). Along with the simplified models, process-based models such as LITPACK and UNIBEST have been used to simulate LST patterns. The long-term net annual LST rate is typically estimated using hydrographic surveys and sediment budget analysis. Although these rough approaches do not provide any information on LST variations in time, they can be used to calibrate sediment transport models. Then the calibrated sediment transport models can be employed to estimate long-term patterns of LST.

This paper provides a preliminary investigation of the uncertainty associated with choice of LST model by comparing the intra- and inter-annual variability of LST patterns projected by a range of models for a short stretch of coastline close to the Gold Coast Seaway (QLD, Australia).

STUDY AREA

The Gold Coast (GC) is a coastal city located in southeast Queensland, Australia (Figure 2a). The GC beaches are social places where people interact, exercise, and relax. The beaches are also a major driver of the local tourism economy. The GC has a 35 km sandy coast (with medium to fine sand-sized grain) backed by a primary dune system. Coastal profiles along the shoreline typically show multiple bars (Figure 2c). The littoral system is interrupted by three natural headlands and four river/creek inlets (Figure 2a). Offshore waves in the region are typically one of five wave climate types (Splinter et al., 2012): long period swells from the S-SE direction, medium-period swells (generated in the Tasman Sea), wind waves from different directions, tropical cyclones (generated in the Coral Sea), and East Coast Lows (ECL) from the NE to SE direction. Coastal erosion along the coast occasionally occurs due to the highly developed coastline lacking a sufficient buffer for major storm events. Hence, to mitigate erosion problems in this region, periodic beach nourishment has been recommended and carried out. Additionally, two sand bypassing systems have been installed at the south and north of the Gold Coast. The sand bypassing systems mitigate the interruption of longshore drift caused by the extension of the training walls of the river entrances, as well as the construction of groins and two artificial reefs. The predominance of waves from the south-easterly direction is recognizable in the offshore wave rose of GC (Figure 2b). The average long-term net northward littoral drift has been estimated to be 500,000 m^3 /year at the southern GC (DHL, 1992) and 635,000 m^3/year at the northern GC (Patterson, 2007). It is worth mentioning that the changes in the LST rate can have significant influences on the rate of beach nourishment and artificial sand bypassing (or sand back-passing) in this study area. The focus of this paper is a 3-km stretch of coastline close to GC Seaway at the northern end of GC (Figure 2a).

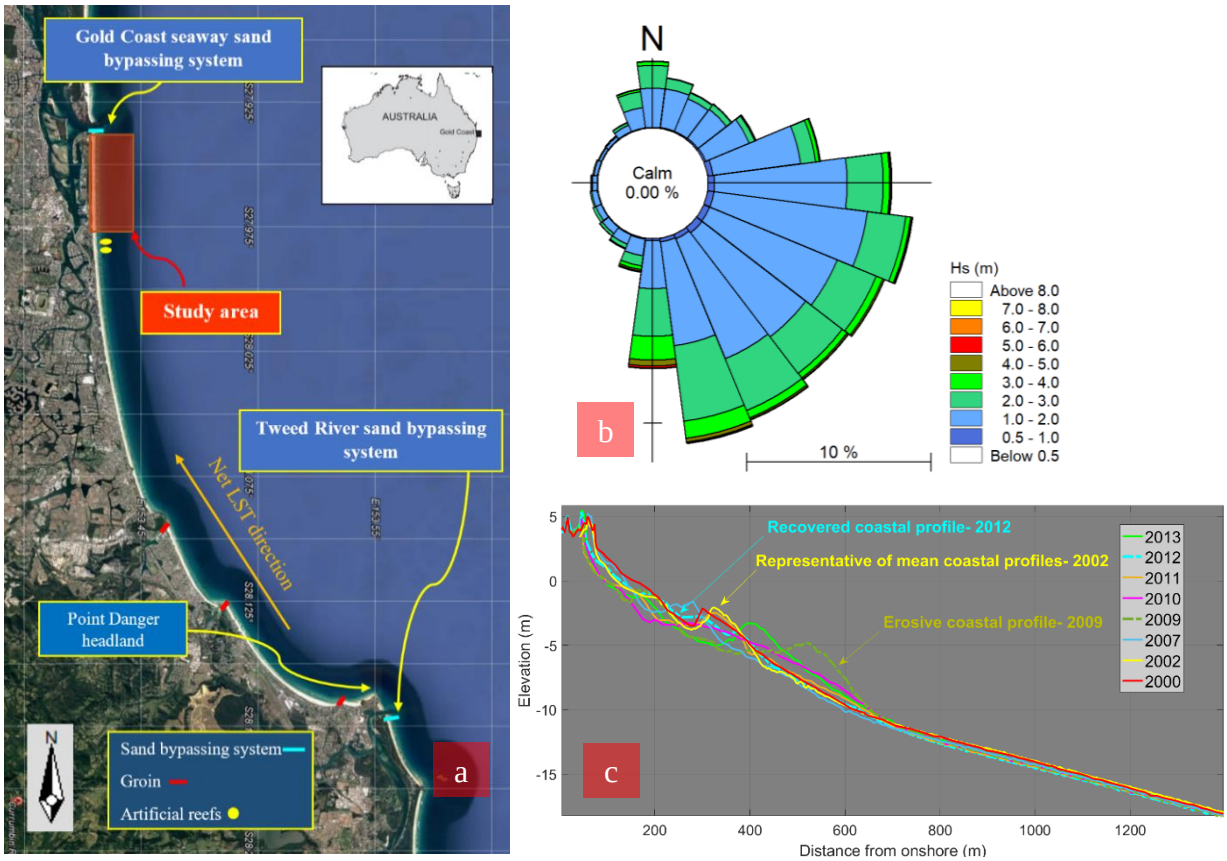

Figure 2. a) Study area; b) offshore wave rose (H_s-D_m obtained from CFSR-driven waves); c) the representative mean coastal profile for North Gold Coast

METHODOLOGY

In this study, the uncertainty associated with choice of LST estimation model was investigated. In this regard, an ensemble of LST models, including Kamphuis (Kamphuis,1991; hereafter K1), modified Kamphuis (Mil-Homens et al., 2013; hereafter K2), CERC (USACE, 1984; hereafter C), Van Rijn (van Rijn, 2014; hereafter V), two new formulas (hereafter S1 and S2) proposed by Shaeri et al. (2020), as well as a process-based model (LITPACK, hereafter DHI) have been used to project the LST rate. Table 1 indicates the dependency of the used transport formulae to different parameters. To set-up LITPACK, a representative mean coastal profile, through analyzing the shape of measured profiles and the corresponding wave climate of northern Gold Coast, was chosen (Figure 2c). To this end, fully recovered coastal profiles (a rare condition for northern GC) or completely erosive ones (one immediately measured after extreme conditions), were excluded from analysis as they could not be representative of long-term shape of coastal profiles.

Table 1. Sensitivity of the transport formulae to different parameters

LST formulae	Dependency to H_b	Dependency to T_p	Dependency to α_b	Dependency to m_b	Dependency to D_{50}
CERC (USACE, 1984)	$\propto H_{sb}^{2.5}$	No	$\propto \sin(2\alpha_b)$	No	No
Kamphuis (Kamphuis, 1991)	$\propto H_{sb}^{2}$	$\propto T_p^{1.5}$	$\propto (\sin 2\alpha_b)^{0.6}$	$\propto m_b^{0.75}$	$\propto D_{50}^{-0.25}$
Modified Kamphuis (Mil-Homens et al., 2013)	$\propto H_{sb}^{2.75}$	$\propto T_p^{0.89}$	$\propto (\sin 2\alpha_b)^{0.5}$	$\propto m_b^{0.86}$	$\propto D_{50}^{-0.69}$
Van Rijn (van Rijn, 2014)	$\propto H_{sb}^{3.1}$	implicitly	$\propto \sin(2\alpha_b)$	$\propto m_b^{0.4}$	$\propto D_{50}^{-0.6}$
Shaeri (Shaeri et al., 2020) (in a dimensional form)	$\propto H_{sb}^{2}$	$\propto T_p^{0.8}$	$\propto (\sin 2\alpha_b)^{0.6}$	implicitly	$\propto D_{50}^{-0.25}$
Shaeri (Shaeri et al., 2020) (in a nondimensional form)	$\propto H_{sb}^{2.3}$	$\propto T_p^{0.8}$	$\propto (\sin 2\alpha_b)^{0.5}$	implicitly	$\propto D_{50}^{-0.2}$

Description: H_{sb} is the significant wave height at breaker point (in m); Tp is peak wave period; α_b is the angle of waves at breaker point (in degree or radian); m_b is the beach slope within surf zone, and D_{50} is the median size of sediment particles (m).

All offshore waves of this study were extracted from the CSIRO's CMIP5 global future wave projections databases (Hemer et al., 2015; Hemer and Trenham, 2016). Nearshore wave forcing conditions were first obtained by applying a simple, low-computational-cost wave transformation method (e.g., Battjes and Stive, 1985, Larson et al., 2010) to the hindcast datasets (CFSR-driven waves) for the period of 1979 to 2005. The depth-induced breaking wave height was estimated using the breaker index (γ_b) of Kamphuis (2010):

$$\gamma_b = {}^{H_{sb}}/_{d_b} = 0.56\, e^{3.5\, m} \qquad (1)$$

where H_{sb} is breaker height, d_b is the water depth at break point, and m is the average surf zone bed slope. All LST models were then calibrated to reproduce the estimated rate of average long-term annual net LST in the area (i.e., 635,000 m^3/year, Patterson, 2007). For calibration of the bulk transport formulas, simple adjustment factors were applied (Table 2); while for calibration of the process-based model, its free parameters were tuned (Table 3). Since shoreline orientation in northern GC has remained in an equilibrium condition in recent decades, it was assumed that shoreline orientation does not change in the future.

Table 2. Settings used for tuning the transport formulae

Formulae	K1	K2	C	V	S1	S2
The correction factor applied to the formulae	0.7	0.9	0.3	0.5	1.5	1.2

D_{50}=0.2 mm
Average surfzone slope= 0.02
The angle of normal to coastline=89 degree

Table 3. Settings used for calibration of the process-based model, LITPACK

D_{50}=0.2 mm
The coastal profile used=a measured profile, representative of mean shape of profiles
The angle of normal to coastline=89 degree
Settling velocity= 0.026 m/s
Bed roughness=0.045 m
Ripple effects: included
Method to calculate wave characteristics across the coastal profile: Battjes and Stive (1985)
Critical Shields parameter=0.05
Description of bedload concentration: deterministic
Wave theory employed for calculation of the orbital wave motion: Doering and Bowen (1995)

To project future LST patterns, offshore waves projected with surface wind forcing from the MRI-CGCM3 GCM was used. This GCM was selected from the eight available GCMs as it provided the best comparison with the wave rose of the CFSR-driven hindcast (not shown). Nearshore wave conditions (the forcing conditions of LST models) for the baseline (1979-2005) and future (2081-2100, under RCP 8.5) periods were obtained using the simple wave transformation method. The ensemble of LST projections was then analyzed to examine the intra- and inter-annual variability of LST and to establish the range of uncertainty corresponding to the choice of LST model. The projected change for each LST model was computed as follows:

$$\Delta_{LST} = \sum_{mo=1}^{n} \left(\frac{\mathrm{LSTF_{mo}} - \mathrm{LSTB_{mo}}}{\mathrm{LSTB_{mo}}} \right) / \mathrm{n} \qquad (2)$$

Where $LSTF_{mo}$ and $LSTB_{mo}$ are the LST rates estimated by the LST model '*mo'* for future and baseline periods, respectively, and *n* is the number of ensemble members (LST models).

RESULTS AND DISCUSSION

The boxplots of CFSR-driven waves (Figure 3, left panel) imply that for the historical period 1979-2005, wave height distribution (i.e., first quartile, median and third quartile) varies monthly. Additionally, the occurrence of storms during February to April intensifies compared to other months. The statistical distribution of wave direction varies considerably from month to month. The rotation of waves direction toward the southeast, from May to August, is recognizable (Figure 3, right panel). This pattern was also observed in MRI-CGCM3-driven waves for the baseline period 1979-2005 (not shown).

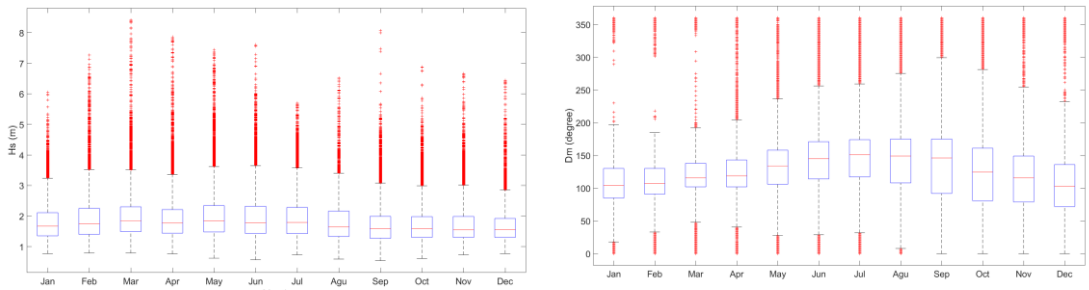

Figure 3. Monthly offshore wave height (left panel) and mean wave direction (right panel) for baseline period 1979-2005 from CFSR-driven waves data

Projected future wave climate of MRI-CGCM-driven waves indicates ~ 5% decrease in mean significant wave height (Figure 4), and 2% decrease in mean peak wave period compared to the baseline period (not shown). Rotation of future wave direction towards the east, particularly from June to September (5 to 10 degrees), is recognizable (Figure 4). Besides, the GCM-driven waves data shows that the H_{s95} and H_{s99} of future waves decrease by 6.5% and 7%, respectively, compared to the baseline period. Therefore, the projected changes in the wave climate could lead to changes in the future patterns of LST.

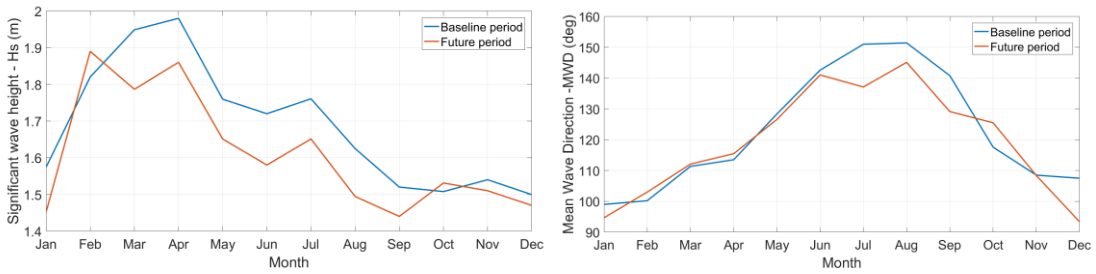

Figure 4. Left: Monthly mean significant wave height for the baseline and future periods (MRI-CGCM3-driven waves); Right: Monthly mean wave direction for the baseline and future periods (MRI-CGCM3-driven waves)

The offshore waves of the studied area are a combination of modal and stormy conditions so each of models were applied during stormy and modal conditions (Figure 5). During stormy conditions, the K1

formula results in the lowest LST rates whilst the process-based model (DHI) and the V formula provide the highest estimates. During modal conditions, the DHI model provides the smallest LST estimates rates. As the process-based model considers sediment transport processes in the forms of both bedload and suspended load, it is conceivable that the relative contributions of bedload and suspended load to the total load are different during extreme and modal conditions. Under extreme wave forcing, the model simulates the separation of more sediments from bed, and as a result, more sediments become available in water column that eventually are transported by strong wave-driven longshore currents. In contrast to the other bulk formulae, the V formula was initially developed based on field measurements, experimental data, and numerical modeling. That is probably why its behavior is closer to that of the process-based model. Nonetheless, since all models were calibrated by long-term average net annual LST rate, instead of relying on the results of a specific model for the prediction of long-term patterns of LST, the mean ensemble of results was considered for projections.

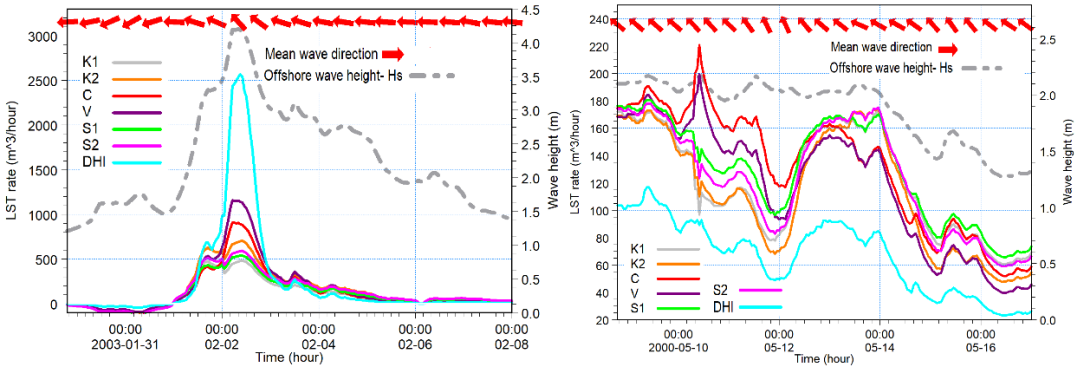

Figure 5. The LST rates obtained from different LST models during a stormy condition (left), and a modal condition (Right)

Figure 6 shows the intra-annual variation of monthly LST amounts for baseline and future periods associated with the forcing of MRI-CGCM3-driven waves. Seasonal variations in LST are observed due to seasonal changes in wave direction, and somehow, due to variations in the wave height. The highlighted gray area shows the range of uncertainty associated with the choice of LST models (inter-model uncertainty). The range of the uncertainty during February to April is really high (~50,000 m^3/month difference in LST rate), whereas during November to January the uncertainty range is meager. The cycle for the baseline period indicates an increase in the LST rate from January to March and a decrease from March to December. This pattern changes slightly in the future period, as the duration of the seasonal cycle of LST is extended to April.

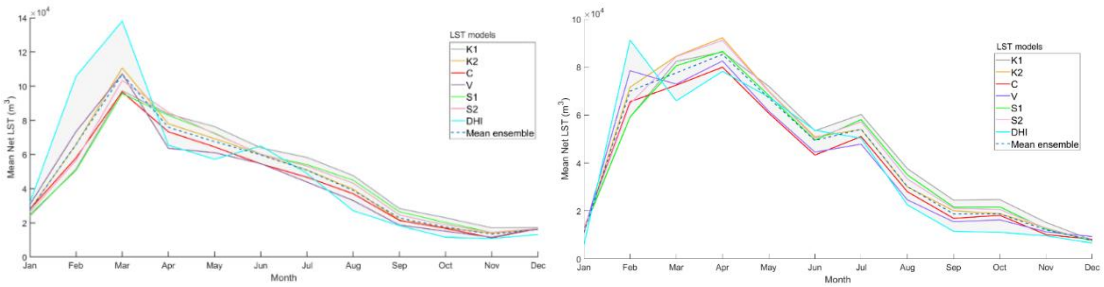

Figure 6. The seasonal cycle of LST rates for the baseline (left figure) and future (right figure) periods

The projected future LST rate shows a decrease in almost all months, compared to the baseline period (variation of LST calculated by each model has been presented in Figure 7 and Figure 8). Each LST model has projected a different magnitude of variations in LST rates. For instance, the DHI model

projected a 19 % decrease in the annual rate of LST, while the S2 formula projected only a 9 % decrease. The mean of results (ensemble mean) shows ~ 11% decrease (compared to the baseline period) in annual and monthly mean LST rate.

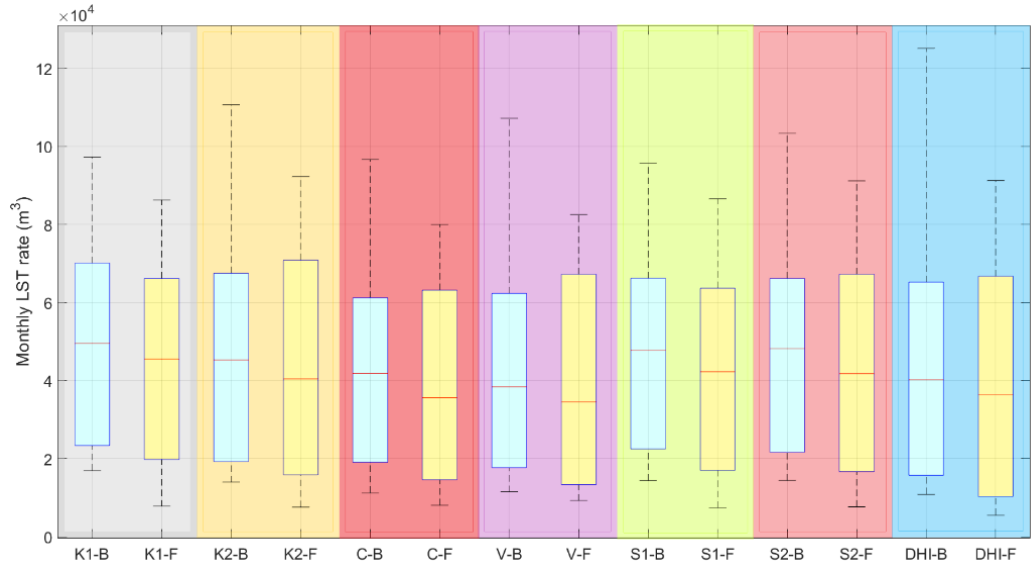

Figure 7. Variation of monthly net LST rate obtained from different models for the baseline (B) and future (F) periods (forcing condition: MRI-CGCM3-driven wave data)

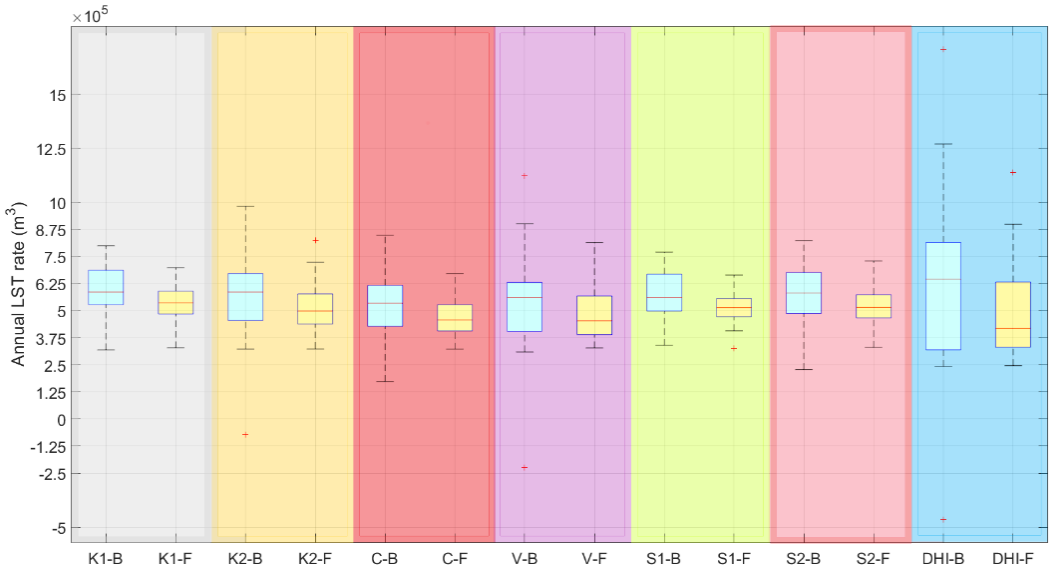

Figure 8. Variation of annual net LST rate for the baseline (B) and future (F) periods (forcing condition: MRI-CGCM3-driven wave data)

Intra- and inter-annual variability of the LST rates were also determined based on normalized standard deviations of the results (i.e., intra-annual variability: standard deviation of the monthly means/time slice mean, inter-annual variability: standard deviation of the annual means/time slice mean); see Table 4. It seems that the DHI and the V models show higher inter-annual variability, compared to other models. But, all model, in the timescale of months, show relatively close intra-annual variability. Whilst there is variance amongst the LST models they are all in qualitative agreement with a projected increase in intra-annual variability and a decrease in the inter-annual variability. Understanding the impact of such

variabilities (estimated by different LST models) on prediction of coastal evolution, and the corresponding countermeasures (e.g., sand bypassing) requires more investigation.

Table 4. Normalized standard deviation of the results

Models	Baseline period 1979-2005		Future period 2081-2100, RCP8.5	
	Intra-annual variability	Inter-annual variability	Intra-annual variability	Inter-annual variability
K1	0.56	0.23	0.63	0.17
K2	0.64	0.36	0.70	0.23
C	0.61	0.30	0.68	0.18
V	0.66	0.45	0.72	0.26
S1	0.58	0.23	0.65	0.16
S2	0.61	0.26	0.68	0.18
DHI	0.81	0.67	0.88	0.48
Ensemble of the LST models	0.64	0.39	0.70	0.26

LIMITATIONS AND THE WAY FORWARD

In this study, inter-model uncertainty was addressed by be employing an ensemble of LST models that were calibrated against a long-term average estimate of the annual LST for the historical period. Choosing the members of the ensemble can be a challenging task. Because forming an ensemble with more transport formulae than process-based models can bias the results of ensemble toward transport formulae limitations. A simple low-computational cost wave transformation method was applied to the offshore forcing as northern GC is far away from headlands and the bathymetry is not complicated. Using the simple wave transformation for other coastal regions of GC (e.g., southern GC) is not justifiable. Hence, a spectral-based wave transformation/hybrid method (e.g., Antolínez et al., 2016, 2018) is preferred at the expense of considerably higher computational costs.

Another limitation of this preliminary study is that the uncertainty associated with the choice of parameters incorporated within each LST model (e.g., beach slope, shoreline orientation, sediment grain diameter, the shape of coastal profiles) have not been considered. Moreover, uncertainties arising from other sources such as emission scenarios, GCMs, and wave transformation methods should be addressed. In this way, the overall reliability (robustness) of projections can be determined. Hence, some other investigations should be conducted to a more sophisticated framework that yields probabilistic results. Such a framework could be developed within coastal management and adaptation plans of the study area.

CONCLUSION

In this paper, a preliminary investigation of the uncertainty associated with the choice of LST model was presented. In this regard, an ensemble of models, including bulk transport formulae and a process-based model, was employed. The forcing conditions of the LST models were obtained from the projected waves of one GCM-forced wave simulation (under one RCP) that were transferred to nearshore using a simple wave transformation method. The results showed that whilst there is variance amongst the results of LST models they are all in qualitative agreement with a projected increase in intra annual variability and a decrease in the inter-annual variability. The mean of results (ensemble mean) shows ~ 11% decrease (compared to the baseline period) in annual and monthly mean LST rate. It should be noted that the results of this study are not still applicable to coastal planning, as other sources of uncertainty should also be considered to find the robustness of projections.

REFERENCES

Almar, R., Kestenare, E., Reyns, J., Jouanno, J., Anthony, E.J., Laibi, R., Hemer, M., Du Penhoat, Y., Ranasinghe, R., 2015. Response of the Bight of Benin (Gulf of Guinea, West Africa) coastline to

anthropogenic and natural forcing, Part1: Wave climate variability and impacts on the longshore sediment transport. Cont. Shelf Res. 110, 48–59. https://doi.org/10.1016/j.csr.2015.09.020

Antolínez, J.A.A., Méndez, F.J., Camus, P., Vitousek, S., González, E.M., Ruggiero, P., Barnard, P., 2016. A multiscale climate emulator for long-term morphodynamics (MUSCLE-morpho). J. Geophys. Res. Ocean. 121, 775–791. https://doi.org/10.1002/2015JC011107

Antolínez, J.A.A., Murray, A.B., Méndez, F.J., Moore, L.J., Farley, G., Wood, J., 2018. Downscaling Changing Coastlines in a Changing Climate: The Hybrid Approach. J. Geophys. Res. Earth Surf. 123, 229–251. https://doi.org/10.1002/2017JF004367

Battjes, J.A., Stive, M.J.F., 1985. Calibration and verification of a dissipation model for random breaking waves. J. Geophys. Res. Ocean. 90, 9159–9167.

Chowdhury, P., Behera, M.R., Reeve, D.E., 2020. Future wave-climate driven longshore sediment transport along the Indian coast. Clim. Change. https://doi.org/10.1007/s10584-020-02693-7

Cooper, J.A.G., Pilkey, O.H., 2007. Field measurement and quantification of longshore sediment transport: an unattainable goal? Geol. Soc. London, Spec. Publ. 274, 37–43. https://doi.org/10.1144/GSL.SP.2007.274.01.05

Dastgheib, A., Reyns, J., Thammasittirong, S., Weesakul, S., Thatcher, M., Ranasinghe, R., 2016. Variations in the wave climate and sediment transport due to climate change along the coast of Vietnam. J. Mar. Sci. Eng. 4. https://doi.org/10.3390/jmse4040086

DHI, 2017. Littoral Processes Module, user guide 1–115.

DHL, 1992. Southern Gold Coast Littoral Sand Supply. Technical Report H85, Delft Hydraulics Laboratory.

Doering, J.C., Bowen, A.J., 1995. Parametrization of orbital velocity asymmetries of shoaling and breaking waves using bispectral analysis. Coast. Eng. 26, 15–33. https://doi.org/10.1016/0378-3839(95)00007-X

Gerhard Masselink, M.G.H., 2003. Introduction to Coastal Processes and Geomorphology, 1st Editio. ed. Routledge. https://doi.org/10.4324/9780203783740

Hanson, H., Kraus, N.C., 1989. GENESIS: Generalized Model for Simulating Shoreline Change. Report 1. Technical Reference.

Hemer, M., Trenham, C., Durrant, T., Greenslade, D., 2015. CAWCR Global wind-wave 21st century climate projections. v2. CSIRO. Service Collection. https://doi.org/https://doi.org/10.4225/08/55C991CC3F0E8

Hemer, M.A., Trenham, C.E., 2016. Evaluation of a CMIP5 derived dynamical global wind wave climate model ensemble. Ocean Model. 103, 190–203. https://doi.org/10.1016/j.ocemod.2015.10.009

Kamphuis, J.W., 2010. Introduction to Coastal Engineering and Management, Advanced Series on Ocean Engineering. WORLD SCIENTIFIC. https://doi.org/10.1142/7021

Kamphuis, J.W., 1991. Alongshore sediment transport rate. J. Waterw. Port, Coastal, Ocean Eng. 117, 624–640. https://doi.org/https://doi.org/10.1061/(ASCE)0733-950X(1991)117:6(624)

Karsten Mangor, Nils K. Drønen, K.H.K. and S.E.K., 2017. Shoreline Management Guidlines - DHI. DHI.

Larson, M., Hoan, L.X., Hanson, H., 2010. Direct formula to compute wave height and angle at incipient breaking. J. Waterw. Port, Coast. Ocean Eng. 136, 119–122. https://doi.org/10.1061/(ASCE)WW.1943-5460.0000030

Mil-Homens, J., Ranasinghe, R., van Thiel de Vries, J.S.M., Stive, M.J.F., 2013. Re-evaluation and improvement of three commonly used bulk longshore sediment transport formulas. Coast. Eng.

75, 29–39. https://doi.org/10.1016/j.coastaleng.2013.01.004

Patterson, D.C., 2007. Sand Transport and Shoreline Evolution , Northern Gold Coast , Australia. Analysis 2007, 147–151.

Ranasinghe, R., 2016. Assessing climate change impacts on open sandy coasts: A review. Earth-Science Rev. 160, 320–332. https://doi.org/10.1016/j.earscirev.2016.07.011

Ruggiero, P., Buijsman, M., Kaminsky, G.M., Gelfenbaum, G., 2010. Modeling the effects of wave climate and sediment supply variability on large-scale shoreline change. Mar. Geol. 273, 127–140. https://doi.org/10.1016/j.margeo.2010.02.008

Shaeri, S., Etemad-Shahidi, A., Tomlinson, R., 2020. Revisiting Longshore Sediment Transport Formulas. J. Waterw. Port, Coastal, Ocean Eng. 146, 04020009. https://doi.org/10.1061/(ASCE)WW.1943-5460.0000557

Splinter, K.D., Davidson, M.A., Golshani, A., Tomlinson, R., 2012. Climate controls on longshore sediment transport. Cont. Shelf Res. 48, 146–156. https://doi.org/10.1016/j.csr.2012.07.018

Toimil, A., Camus, P., Losada, I.J., Le Cozannet, G., Nicholls, R.J., Idier, D., Maspataud, A., 2020. Climate change-driven coastal erosion modelling in temperate sandy beaches: Methods and uncertainty treatment. Earth-Science Rev. 202, 103110. https://doi.org/10.1016/j.earscirev.2020.103110

Tonnon, P.K., Huisman, B.J.A., Stam, G.N., van Rijn, L.C., 2018. Numerical modelling of erosion rates, life span and maintenance volumes of mega nourishments. Coast. Eng. 131, 51–69. https://doi.org/10.1016/j.coastaleng.2017.10.001

USACE, 1984, 1984. Shore protection manual /[prepared for Department of the Army, US Army Corps of Engineers]. Vicksburg, Miss. :Dept. of the Army, Waterways Experiment Station, Corps of Engineers, Coastal Engineering Research Center ; https://doi.org/https://doi.org/10.5962/bhl.title.47829

van Rijn, L.C., 2014. A simple general expression for longshore transport of sand, gravel and shingle. Coast. Eng. 90, 23–39. https://doi.org/10.1016/j.coastaleng.2014.04.008

Van Rijn, L.C., 1998. Principles of coastal morphology.